

Luminescence of Ln(III) Dithiocarbamate Complexes (Ln = La, Pr, Sm, Eu, Gd, Tb, Dy)

Michelle D. Regulacio, Michele H. Pablico, Joan Acay Vasquez,[†] Peter N. Myers, Stuart Gentry,[§] Michael Prushan,[§] Suk-Wah Tam-Chang,[†] and Sarah L. Stoll*

Department of Chemistry, Georgetown University, Washington D.C. 20057

Received October 5, 2007

We have discovered room temperature photoluminescence in Sm³⁺ and Pr³⁺ dithiocarbamate complexes. Surprisingly, these complexes exhibit more intense emission than those of the Eu³⁺, Tb³⁺, and Dy³⁺ analogues. The electronic absorption, excitation, and emission spectra are reported for the complexes [Ln(S₂CNR₂)₃L] and NH₂Et₂[Ln(S₂CNEt₂)₄], where Ln = Sm, Pr; R = ethyl, *t*-butyl, benzyl; and L = 1,10-phenanthroline, 2,2'-bipyridine, and 5-chloro-1,10-phenanthroline. The lowest ligand-localized triplet energy level (T₁) of the complexes are determined from the phosphorescence spectra of analogous La³⁺ and Gd³⁺ chelates. The luminescence decay curves were measured to determine the excited-state lifetimes for the Pr³⁺ and Sm³⁺ complexes. X-ray crystal structures of Sm(S₂CN*t*Bu₂)₃phen, Pr(S₂CNEt₂)₃phen, and Pr(S₂CN*t*Bu₂)₃phen are also reported.

Introduction

Synthesis of luminescent lanthanide complexes has been of considerable interest because of their potential applications, such as fluorescent labeling reagents, imaging agents, and emitter materials in organic light-emitting diodes (OLEDs).^{1–3} Generally, complexes of Eu³⁺, Sm³⁺, Tb³⁺, and Dy³⁺ are considered to have the brightest emission, but the luminescence efficiency of these complexes largely depends on the choice of organic ligands.⁴ Since the forbidden f–f transitions make direct photoexcitation of lanthanide ions unfavored, the organic ligands function like an antenna by absorbing light and transferring this energy to the excited states of the central lanthanide ion. The excited lanthanide ion then undergoes radiative transitions to lower energy states resulting in characteristic multiple narrow-band emissions. Since the intensity of the emission (brightness) and choice of lanthanide (i.e., color of emission) both depend on the sensitizer, new sensitizing chromophores are highly sought after.⁵

Several nitrogen- and oxygen-donor ligands have been utilized in the sensitization of lanthanide luminescence. In particular, bidentate aromatic amines, carboxylic acids, and β-diketonates are known to provide efficient energy transfer to lanthanide ions.^{6–8} However, very little has been reported on the luminescence of sulfur-coordinated lanthanide chelates. This may be due to the generally low stability of complexes that form between hard lanthanides and soft sulfur-donor ligands. Our group has developed the use of bidentate monoanionic dithiocarbamates RR'NCS₂[−] (where R, R' = alkyl groups) to prepare air-stable sulfur-bound lanthanide complexes. These ligands can be coordinated to lanthanides to form anionic complexes, [Ln(S₂CNR₂)₄][−],^{9–14} or neutral complexes, Ln(S₂CNR₂)₃.¹⁰ Stable complexes of

* Author to whom correspondence should be addressed. E-mail: sls55@georgetown.edu. Fax: 202-687-6209. Tel.: 202-687-5839.

[†] Department of Chemistry, University of Nevada, Reno, NV 89557.

[§] Department of Chemistry and Biochemistry, La Salle University, Philadelphia, PA 19141.

- (1) Frias, J. C.; Bobba, G.; Cann, M. J.; Hutchinson, C. J.; Parker, D. *Org. Biomol. Chem.* **2003**, *1*, 905–907.
- (2) Diaz-Garcia, M. A.; De Avila, S. F.; Kuzyk, M. G. *Appl. Phys. Lett.* **2002**, *81*, 3924–3926.
- (3) Duan, J.-P.; Sun, P.-P.; Cheng, C.-H. *J. Mater. Online* **2005**, *1*.
- (4) Crosby, G. A.; Whan, R. E.; Freeman, J. J. *J. Phys. Chem.* **1962**, *66*, 2493–2499.

(5) Pope, S.; Coe, B. J.; Faulkner, S.; Bichenkova, E. V.; Yu, X.; Douglas, K. T. *J. Am. Chem. Soc.* **2004**, *126*, 9490.

(6) Yan, B.; Zhang, H. J.; Wang, S. B.; Ni, J. Z. *Spectrosc. Lett.* **1998**, *31*, 603.

(7) Yan, B.; Song, Y. S. *J. Fluor.* **2004**, *14*, 289–294.

(8) Sato, S.; Wada, M. *Bull. Chem. Soc. Jpn.* **1970**, *43*, 1955–1962.

(9) Kobayashi, T.; Naruke, H.; Yamase, T. *Chem. Lett.* **1997**, *26*, 907–908.

(10) Brown, D.; Holah, D. G.; Rickard, C. E. F. *J. Chem. Soc. A* **1970**, 786–790.

(11) Siddall, T. H. I.; Stewart, W. E. *J. Inorg. Nucl. Chem.* **1970**, *32*, 1147–1158.

(12) Su, C.-Y.; Tang, N.; Tan, M.-Y.; Gan, X.-M.; Cai, L.-P. *Synth. React. Inorg. Met.-Org. Chem.* **1997**, *27*, 291–300.

(13) Ciampolini, M.; Nardi, N.; Colamarino, P.; Orioli, P. *J. Chem. Soc., Dalton Trans.* **1977**, 379–384.

(14) Su, C.-Y.; Tan, M.-Y.; Tang, N.; Gan, X.-M.; Zhang, Z.-F.; Xue, Q.-J.; Yu, K.-B. *Polyhedron* **1997**, *16*, 1643–1650.

lanthanide dithiocarbamates with a neutral bidentate ligand, L (usually 1,10-phenanthroline or 2,2'-bipyridine), having the general formula, $\text{Ln}(\text{S}_2\text{CNR}_2)_3\text{L}$, have also been reported.^{15–19} These complexes can be conveniently prepared in air, many can be made in water, and most crystallize easily.

Recent studies on lanthanide dithiocarbamates focus mainly on their thermal properties because of their potential utility as precursors for the fabrication of lanthanide sulfide nanoparticles and thin films.^{15,20–27} Their photoluminescence properties, on the other hand, are hardly investigated. Among the lanthanide dithiocarbamates reported, only those of Eu^{3+} have been studied for their photoluminescence properties. First to be reported was the observed photoluminescence of $\text{Na}[\text{Eu}(\text{S}_2\text{CN}(\text{CH}_3)_2)_4 \cdot 3.5\text{H}_2\text{O}]$ at 4.2 K.⁹ More recently, room temperature luminescence was reported for the complexes very close in structure to those reported here, $\text{Eu}(\text{S}_2\text{CNET}_2)_3\text{phen}$, $\text{Eu}(\text{S}_2\text{CNET}_2)_3\text{bipy}$, and $\text{Eu}(\text{S}_2\text{CNPh}_2)_3\text{phen}$.²⁸ The preference for studying the photoluminescence of europium complexes is not surprising. Of all the rare-earth complexes, those with Eu^{3+} are the most thoroughly investigated due to the trivalent europium ion's characteristic strong red emission, which can be exploited in electroluminescent devices as well as in fluorescent assay of biomolecules, which autofluoresce in the blue region of the spectrum. Chelates of Sm^{3+} and Pr^{3+} , by contrast, have received far less attention particularly the chelates of Pr^{3+} because of their relatively low luminescence intensity.

In this paper, the photoluminescence properties of Sm^{3+} and Pr^{3+} dithiocarbamates at room temperature are studied for the first time. Remarkably, the luminescence efficiency of these complexes is greater than those of the previously reported Eu^{3+} dithiocarbamates, and greater than two other potentially bright emitters, the Tb^{3+} and Dy^{3+} analogues. The dithiocarbamate ligands are special in sensitizing Pr^{3+} , which is of interest for its potential to emit not only in the visible

but also in the NIR region, a range important for fiber optics and telecommunications.²⁹ The effect of varying the neutral bidentate ligand (L), the alkyl group (R) of the dithiocarbamate ligand, and the ligand ratio (dtc:L) on the photoluminescence of these compounds is investigated.

Experimental Section

General Information. The dithiocarbamate ligands, with the exception of diethylammonium diethyldithiocarbamate, were prepared using a modified version of previously published procedures.³⁰ Diethylammonium diethyldithiocarbamate, carbon disulfide, tetramethylammonium hydroxide, diisobutylamine, dibenzylamine, 1,10-phenanthroline, 2,2'-bipyridine, 5-chloro-1,10-phenanthroline, and the rare-earth salts were purchased from Aldrich Chemical Co. and used as received. NMR spectra were recorded using a 300 MHz Bruker spectrometer, calibrated internally to residual solvent for ^1H in CDCl_3 . Infrared spectra were measured in the range 450–4000 cm^{-1} as pressed pellets in KBr on a Perkin-Elmer Spectrum One FTIR spectrometer. Absorption spectra were recorded from 210 to 800 nm in acetonitrile on a Perkin-Elmer Lambda 35 UV-visible spectrometer.

Steady-state, room temperature luminescence measurements were conducted using a Jobin Yvon-SPEX FluoroMax-2 fluorometer with a 150 W xenon source and a Hamamatsu R928P PMT. For emission spectra, 7 nm slit widths were used, with a scan speed of 80 nm/min. All excitation and emission spectra were corrected for the sensitivity of the detector and wavelength dependence of the output power of the source. Phosphorescence spectra of the Gd^{3+} and La^{3+} complexes were measured at liquid nitrogen temperature (77 K) using a Jobin Yvon FluoroLog 3-222 spectrofluorometer with a 450 W xenon lamp as the excitation source.

Lifetime measurements were carried out on N_2 purged acetonitrile solutions of $\text{Sm}(\text{S}_2\text{CNET}_2)_3\text{phen}$ and $\text{Pr}(\text{S}_2\text{CNET}_2)_3\text{phen}$ contained in quartz cuvettes. The samples were excited with a 337 nm VSL337 20 kW peak power, 3 ns duration, and 20 pps nitrogen laser (Laser Science, Inc. Franklin, MA), and the luminescence was detected by a photomultiplier tube operating at 0.8 kV. A portion of the excitation pulse was reflected off of a glass plate placed at a 45° angle in the laser beam path onto a photodiode. A 337 nm cutoff filter was placed in the laser excitation path to attenuate the intensity. The sample emission was filtered with orange glass and 600 nm cutoff filters to reduce scattered laser light. The electric pulses generated by the photodiode and photomultiplier tube were sent to a Hewlett-Packard 54504A digitizing oscilloscope interfaced to a computer. An average of 200 waveforms was collected using a program written with Labview (National Instruments, Austin, TX). The decay curves were analyzed via a nonlinear least-squares fitting routine using the Origin 6.0 software package.

Relative quantum yields were calculated using the equation: $Q_s/Q_r = (A_r)(n_s^2)(I_s)/(A_s)(n_r^2)(I_r)$ where r stands for the reference (quinine bisulfate in 0.1 N H_2SO_4 , $\Phi = 54.6\%$ at $\lambda_{\text{exc}} = 340$ nm) and s stands for sample. In this equation, A is the absorbance at the excitation wavelength, n is the index of refraction of the solvent, and I is the integrated luminescence intensity. Samples were measured at 6.45×10^{-4} M, to avoid complex dissociation but minimize absorbance. For the determination of the quantum yield, the excitation wavelength was chosen so that $A < 0.05$.

$\text{Sm}(\text{S}_2\text{CNET}_2)_3\text{phen}$, 1. A solution of diethylammonium diethyldithiocarbamate (0.33 g, 1.5 mmol) and 1,10-phenanthroline (0.09

- (15) Regulacio, M. D.; Tomson, N.; Stoll, S. L. *Chem. Mater.* **2005**, *17*, 3114–3121.
- (16) Su, C.-Y.; Tan, M.-Y.; Tang, N.; Gan, X.-M.; Liu, W.-S. *J. Coord. Chem.* **1996**, *38*, 207–218.
- (17) Varand, V. L.; Glinskaya, L. A.; Klevtsova, R. F.; Larionov, S. V. *J. Struct. Chem.* **2000**, *41*, 544–549.
- (18) Su, C.-Y.; Tan, M.-Y.; Zhang, Z.-F.; Tang, N.; Cai, L.-P.; Xue, Q.-J. *Synth. React. Inorg. Met.-Org. Chem.* **1999**, *29*, 35–51.
- (19) Varand, V. L.; Glinskaya, L. A.; Klevtsova, R. F.; Larionov, S. V. *J. Struct. Chem.* **1998**, *39*, 244–252.
- (20) Hasegawa, Y.; Afzaal, M.; O'Brien, P.; Wada, Y.; Yanagida, S. *Chem. Commun.* **2005**, 242–243.
- (21) Mirkovic, T.; Hines, M. A.; Nair, P. S.; Scholes, G. D. *Chem. Mater.* **2005**, *17*, 3451–3456.
- (22) Zhao, F.; Sun, H.-L.; Gao, S.; Su, G. *J. Mater. Chem.* **2005**, *15*, 4209–4214.
- (23) Domrachev, G. A.; Zav'yalova, L. V.; Svechnikov, G. S.; Suvorova, O. N.; Khanova, A. V.; Shchupak, E. A.; Yarosh, L. A. *Russ. J. Gen. Chem.* **2003**, *73*, 560–565.
- (24) Regulacio, M. D.; Bussmann, K.; Lewis, B.; Stoll, S. L. *J. Am. Chem. Soc.* **2006**, *128*, 11173–11179.
- (25) Ivanov, R. A.; Korsakov, I. E.; Formanovskii, A. A.; Paramonov, S. E.; Kuz'mina, N. P.; Kaul', A. R. *Russ. J. Coord. Chem.* **2002**, *28*, 670–672.
- (26) Kuz'mina, N. P.; Ivanov, R. A.; Paramonov, S. E.; Martynenko, L. I. *Proc. Electrochem. Soc.* **1997**, 97–25, 880–885.
- (27) Ivanov, R. A.; Korsakov, I. E.; Kuz'mina, N. P.; Kaul', A. R. *Mendeleev. Commun.* **2000**, *3*, 98–99.
- (28) Faustino, W. M.; Malta, O. L.; Teotonio, E. E. S.; Brito, H. F.; Simas, A. M.; de Sa, G. F. *J. Phys. Chem. A* **2006**, *110*, 2510–2516.

(29) Bunzli, J. G.; Piguet, C. *Chem. Soc. Rev.* **2005**, *34*, 1048–1077.

(30) Thorn, G. D.; Ludwig, R. A. *The Dithiocarbamates and Related Compounds*; Elsevier: New York, 1962.

g, 0.50 mmol) in CH₃CN (10 mL) was added to a solution of SmCl₃ (0.13 g, 0.50 mmol) in H₂O (3 mL). Light yellow crystals came out upon stirring. The solid was isolated through vacuum filtration and then recrystallized from hot CH₃CN. ¹H NMR: δ 1.19 (t, *J* = 7.1 Hz, 18H), δ 3.92 (q, *J* = 7.0 Hz, 12H), δ 7.41 (m, 2H), δ 7.85 (s, 2H), δ 8.29 (m, 4H). IR (KBr, cm⁻¹): ν_{C-N} = 1482(s), ν_{C-S} = 999(m), ν_{phen} = 1623, 1589, 1571, 843, 731. Anal. Calcd. for C₂₇H₃₈N₅S₆Sm: C, 41.82; H, 4.94; N, 9.03; S, 24.82. Found: C, 40.04; H, 5.02; N, 8.71; S, 23.35. Percent yield 82%.

Sm(S₂CNⁱBu₂)₃phen, 2. To a 3 mL aqueous solution of SmCl₃ (0.13 g, 0.50 mmol), a solution of tetramethylammonium diisobutylthiocarbamate (0.42 g, 1.5 mmol) and 1,10-phenanthroline (0.09 g, 0.50 mmol) in 5:1 CH₃CN:MeOH (12 mL) was added. The light yellow solid that immediately came out was isolated. Recrystallization from hot CH₃CN gave bright yellow crystals. ¹H NMR: δ 0.87 (d, *J* = 6.6 Hz, 36H), δ 2.37 (m, *J* = 6.6 Hz, 6H), δ 3.81 (d, *J* = 7.5 Hz, 12H), δ 7.43 (m, 2H), δ 7.83 (s, 2H), δ 8.28 (d, *J* = 8.1 Hz, 2H), δ 8.48 (d, 2H). IR (KBr, cm⁻¹): ν_{C-N} = 1465(s), ν_{C-S} = 989(m), ν_{phen} = 1626, 1589, 1573, 844, 728. Anal. Calcd. for C₃₉H₆₂N₅S₆Sm: C, 49.63; H, 6.62; N, 7.42; S, 20.39. Found: C, 49.54; H, 6.60; N, 7.97; S, 19.94. Percent yield 81%.

Sm(S₂CNBz₂)₃phen, 3. A solution of tetramethylammonium dibenzylthiocarbamate (1.04 g, 3.0 mmol) and 1,10-phenanthroline (0.18 g, 1.0 mmol) in 3:1 CH₃CN:MeOH (20 mL) was added to a solution of Sm(NO₃)₃·6H₂O (0.45 g, 1.0 mmol) in CH₃CN (5 mL). The pale yellow solid that came out was collected, and was then recrystallized from 3:1 CH₃CN:CHCl₃. ¹H NMR: δ 5.27 (s, 12H), δ 7.25 (m, 30H), δ 7.50 (m, 2H), δ 7.98 (s, 2H), δ 8.26 (d, 2H), δ 8.44 (d, *J* = 7.8 Hz, 2H). IR (KBr, cm⁻¹): ν_{C-N} = 1450(s), ν_{C-S} = 991(s), ν_{phen} = 1625, 1589, 1575, 844, 728. Anal. Calcd. for C₅₇H₅₀N₅S₆Sm: C, 59.64; H, 4.39; N, 6.10; S, 16.76. Found: C, 59.09; H, 4.22; N, 5.99; S, 16.59. Percent yield 76%.

Sm(S₂CNEt₂)₃bipy, 4. To an acetonitrile solution (5 mL) of Sm(NO₃)₃·6H₂O (0.45 g, 1.0 mmol), a solution of diethylammonium diethylthiocarbamate (0.67 g, 3.0 mmol) and 2,2'-bipyridine (0.16 g, 1.0 mmol) in CH₃CN (5 mL) was added. Pale yellow solid appeared upon stirring the mixture. The product was collected and then recrystallized using hot CH₃CN. ¹H NMR: δ 1.25 (t, *J* = 7.1 Hz, 18H), δ 3.98 (q, *J* = 7.0 Hz, 12H), δ 6.99 (m, 2H), δ 7.11 (s, 2H), δ 7.87 (t, *J* = 7.7 Hz, 2H), δ 8.15 (d, *J* = 7.5 Hz, 2H). IR (KBr, cm⁻¹): ν_{C-N} = 1483(s), ν_{C-S} = 997(m), ν_{bpy} = 1627, 1594, 1566, 771. Anal. Calcd. for C₂₅H₃₈N₅S₆Sm: C, 39.96; H, 5.10; N, 9.32; S, 25.61. Found: C, 39.42; H, 5.05; N, 9.13; S, 26.11. Percent yield 80%.

Sm(S₂CNEt₂)₃cphen, 5. To an acetonitrile solution (5 mL) of Sm(NO₃)₃·6H₂O (0.45 g, 1.0 mmol), a solution of diethylammonium diethylthiocarbamate (0.67 g, 3.0 mmol) and 5-chloro-1,10-phenanthroline (0.21 g, 1.0 mmol) in 15:1 CH₃CN:MeOH (16 mL) was added. While stirring the mixture, 10 mL H₂O was added, yielding pale yellow solid. The solid was isolated through vacuum filtration. ¹H NMR: δ 1.23 (t, *J* = 6.5 Hz, 18H), δ 3.96 (q, *J* = 7.0 Hz, 12H), δ 7.49 (m, 2H), δ 8.01 (s, 1H), δ 8.24 (m, 3H), δ 8.74 (d, *J* = 8.1 Hz, 1H). IR (KBr, cm⁻¹): ν_{C-N} = 1481(s), ν_{C-S} = 999(s), ν_{cphen} = 1615, 1600, 1589, 1573, 734. Anal. Calcd. for C₂₇H₃₇N₅ClS₆Sm: C, 40.04; H, 4.61; N, 8.65; Cl, 4.38; S, 23.76. Found: C, 38.39; H, 4.40; N, 8.21; Cl, 5.31; S, 22.58. Percent Yield 83%.

NH₂Et₂[Sm(S₂CNEt₂)₄], 6. An isopropanol solution (7 mL) of diethylammonium diethylthiocarbamate (0.45 g, 2.0 mmol) was added to an isopropanol solution (3 mL) of Sm(NO₃)₃·6H₂O (0.22 g, 0.50 mmol). Pale yellow crystals immediately appeared after mixing. The product was isolated through vacuum filtration. ¹H NMR: δ 1.26 (t, *J* = 7.1 Hz, 24H), δ 2.89 (q, *J* = 7.2 Hz, 16H).

IR (KBr, cm⁻¹): ν_{C-N} = 1484(s), ν_{C-S} = 1002(m). Anal. Calcd. for C₂₄H₅₂N₅S₆Sm: C, 35.25; H, 6.41; N, 8.57; S, 31.38. Found: C, 33.95; H, 6.21; N, 8.28; S, 30.85. Percent yield 78%.

Pr(S₂CNEt₂)₃phen, 7. A solution of diethylammonium diethylthiocarbamate (0.67 g, 3.0 mmol) and 1,10-phenanthroline (0.18 g, 1.0 mmol) in CH₃CN (15 mL) was added to a 10 mL CH₃CN solution of Pr(NO₃)₃·6H₂O (0.44 g, 1.0 mmol). Apple green crystals immediately formed upon stirring. The crystals were isolated by vacuum filtration and recrystallized from hot CH₃CN. ¹H NMR: δ 1.97 (t, *J* = 6.9 Hz, 18H), δ 6.01 (q, *J* = 6.9 Hz, 12H), δ -4.74 (s, 2H), δ 5.76 (d, *J* = 8.1 Hz, 2H), δ 8.42 (s, 2H), δ 8.66 (d, *J* = 8.1 Hz, 2H). IR (KBr, cm⁻¹): ν_{C-N} = 1481(s), ν_{C-S} = 996(m), ν_{phen} = 1623, 1589, 1572, 843, 730. Anal. Calcd. for C₂₇H₃₈N₅S₆Pr: C, 42.34; H, 5.00; N, 9.15; S, 25.12. Found: C, 42.08; H, 4.89; N, 8.94; S, 24.93. Percent yield 74%.

Pr(S₂CNⁱBu₂)₃phen, 8. A solution of tetramethylammonium diisobutylthiocarbamate (0.42 g, 1.5 mmol) and 1,10-phenanthroline (0.09 g, 0.5 mmol) in 5:1 CH₃CN:CH₃OH (20 mL) was added to a 10 mL CH₃CN solution of Pr(NO₃)₃·6H₂O (0.22 g, 0.5 mmol). This resulted in the immediate formation of lime green crystals, which were then isolated by vacuum filtration and recrystallized from hot ethanol. ¹H NMR: δ 1.45 (d, *J* = 6.3 Hz, 36H), δ 3.73 (m, *J* = 6.5 Hz, 6H), δ 6.16 (d, *J* = 7.2 Hz, 12 H), δ -4.07 (s, 2H), δ 5.61 (d, *J* = 8.1 Hz, 2H), δ 7.90 (s, 2H), δ 8.24 (d, *J* = 7.8 Hz, 2H). IR (KBr, cm⁻¹): ν_{C-N} = 1472(s), ν_{C-S} = 989(s), ν_{phen} = 1625, 1589, 1573, 847, 729. Anal. Calcd. for C₃₉H₆₂N₅S₆Pr: C, 50.13; H, 6.69; N, 7.50; S, 20.60. Found: C, 49.60; H, 6.58; N, 7.35; S, 20.93. Percent yield 85%.

Pr(S₂CNBz₂)₃phen, 9. A solution of tetramethylammonium dibenzylthiocarbamate (1.04 g, 3.0 mmol) and 1,10-phenanthroline (0.18 g, 1.0 mmol) in 3:1 CH₃CN:MeOH (20 mL) was added to a solution of Pr(NO₃)₃·6H₂O (0.44 g, 1.0 mmol) in CH₃CN (5 mL). The pale green solid that came out was collected, and was then recrystallized from 3:1 CH₃CN:CHCl₃. ¹H NMR: δ 7.24 (s, 12H), δ 7.32 (m, 18H), δ 7.91 (m, 12H), δ -4.83 (s, 2H), δ 5.84 (d, *J* = 8.4 Hz, 2H), δ 8.49 (s, 2H), δ 8.75 (d, *J* = 8.1 Hz, 2H). IR (KBr, cm⁻¹): ν_{C-N} = 1450(s), ν_{C-S} = 991(s), ν_{phen} = 1624, 1589, 1575, 844, 728. Anal. Calcd. for C₅₇H₅₀N₅S₆Pr: C, 60.14; H, 4.43; N, 6.15; S, 16.90. Found: C, 59.70; H, 4.29; N, 6.05; S, 16.79. Percent yield 72%.

Pr(S₂CNEt₂)₃bipy, 10. A solution of diethylammonium diethylthiocarbamate (0.67 g, 3.0 mmol) and 2,2'-bipyridine (0.16 g, 1.0 mmol) in 10 mL CH₃CN was added to a 5 mL CH₃CN solution of Pr(NO₃)₃·6H₂O (0.44 g, 1.0 mmol). Light mint green crystals appeared upon stirring for a few minutes. The crystals were isolated and recrystallized from hot acetonitrile. ¹H NMR: δ 2.14 (t, *J* = 6.9 Hz, 18H), δ 6.27 (q, *J* = 6.9 Hz, 12H), δ -11.79 (s, 2H), δ 4.35 (d, *J* = 7.5 Hz, 2H), δ 7.90 (t, 7.8 Hz, 2H), δ 9.32 (d, *J* = 7.8 Hz, 2H). IR (KBr, cm⁻¹): ν_{C-N} = 1482(s), ν_{C-S} = 995(s), ν_{bpy} = 1624, 1594, 1567, 771. Anal. Calcd. for C₂₅H₃₈N₅S₆Pr: C, 40.47; H, 5.16; N, 9.44; S, 25.93. Found: C, 39.96; H, 5.06; N, 9.32; S, 26.16. Percent yield 60%.

Pr(S₂CNEt₂)₃cphen, 11. To an acetonitrile solution (5 mL) of Pr(NO₃)₃·6H₂O (0.44 g, 1.0 mmol), a solution of diethylammonium diethylthiocarbamate (0.67 g, 3.0 mmol) and 5-chloro-1,10-phenanthroline (0.21 g, 1.0 mmol) in 15:1 CH₃CN:MeOH (16 mL) was added. Yellow green solid came out upon stirring for a few minutes. The solid was isolated and then recrystallized from hot acetonitrile. ¹H NMR: δ 2.13 (t, *J* = 7.1 Hz, 18H), δ 6.29 (q, *J* = 6.9 Hz, 12H), δ -7.09 (s, 1H), δ -5.46 (s, 1H), δ 5.18 (d, 1H), δ 5.56 (d, 1H), δ 8.20 (s, 1H), δ 8.38 (d, *J* = 8.1 Hz, 1H), δ 8.56 (d, *J* = 7.5 Hz, 1H). IR (KBr, cm⁻¹): ν_{C-N} = 1482(s), ν_{C-S} = 997(s), ν_{cphen} = 1615, 1600, 1589, 1573, 734. Anal. Calcd. for

Table 1. Covalency Parameters for the Sm³⁺ and Pr³⁺ Complexes

Sm(III) Complexes			
	β	δ	$b^{1/2}$
Sm(S ₂ CNEt ₂) ₃ phen	0.9905(3)	0.9586(311)	0.06890(111)
Sm(S ₂ CN ⁱ Bu ₂) ₃ phen	0.9906(3)	0.9520(286)	0.06867(103)
Sm(S ₂ CNBz ₂) ₃ phen	0.9911(3)	0.8960(275)	0.06663(102)
Sm(S ₂ CNEt ₂) ₃ bipy	0.9906(3)	0.9520(286)	0.06867(103)
Sm(S ₂ CNEt ₂) ₃ cphen	0.9906(3)	0.9540(306)	0.06874(110)
[Sm(S ₂ CNEt ₂) ₄] [−]	0.9877(3)	1.245(27)	0.07842(83)
Pr(III) complexes			
	β	δ	$b^{1/2}$
Pr(S ₂ CNEt ₂) ₃ phen	0.9739(2)	2.680(24)	0.1142(5)
Pr(S ₂ CN ⁱ Bu ₂) ₃ phen	0.9741(4)	2.657(42)	0.1138(9)
Pr(S ₂ CNBz ₂) ₃ phen	0.9745(4)	2.619(39)	0.1130(8)
Pr(S ₂ CNEt ₂) ₃ bipy	0.9745(4)	2.621(39)	0.1130(8)
Pr(S ₂ CNEt ₂) ₃ cphen	0.9738(6)	2.686(60)	0.1144(13)
[Pr(S ₂ CNEt ₂) ₄] [−]	0.9705(6)	3.044(58)	0.1215(11)

C₂₇H₃₇N₅ClS₆Pr: C, 40.51; H, 4.66; N, 8.75; Cl, 4.43; S, 24.04. Found: C, 40.48; H, 4.76; N, 8.84; Cl, 5.17; S, 23.53. Percent yield 73%.

NH₂Et₂[Pr(S₂CNEt₂)₄], 12. An ethanol solution (15 mL) of diethylammonium diethyldithiocarbamate (0.89 g, 4.0 mmol) was added to an ethanol solution (5 mL) of Pr(NO₃)₃·6H₂O (0.44 g, 1.0 mmol). Pale mint green crystals appeared after stirring the mixture for a few minutes. The product was isolated through vacuum filtration. ¹H NMR: δ 1.16 (t, J = 7.2 Hz, 24H), δ 2.72 (q, J = 7.1 Hz, 16H). IR (KBr, cm^{−1}): ν_{C-N} = 1476(s), ν_{C-S} = 1002(s). Anal. Calcd. for C₂₄H₅₂N₅S₈Pr: C, 35.67; H, 6.49; N, 8.67; S, 31.75. Found: C, 35.15; H, 6.35; N, 8.57; S, 32.09. Percent yield 83%.

Detailed synthetic procedure for the La³⁺, Gd³⁺, Eu³⁺, Tb³⁺, and Dy³⁺ complexes are provided in the Supporting Information.

X-ray Crystallography. Intensity data were collected on a Bruker SMART 1000 CCD diffractometer using Mo K α radiation (λ = 0.71073 Å). The data were integrated using the SAINT suite of software, and absorption corrections were calculated using SADABS. Crystal structures were solved and refined using the SHELX-86 and -97 packages, with the assistance of X-Seed. The structures were solved using direct methods and refined by full-matrix least-squares methods with anisotropic thermal parameters for all nonhydrogen atoms. Hydrogen atoms were located in calculated positions and refined isotropically. The experimental details of the data collections are summarized in Table S1. Complete crystallographic details are also provided in the Supporting Information.

Results and Discussion

Crystal Structures. The crystal structures of some of the complexes studied here were already reported in previous papers.^{15,17,31} In this paper, we report the crystal structures of complexes Sm(S₂CNⁱBu₂)₃phen (**2**), Pr(S₂CNEt₂)₃phen (**7**), and Pr(S₂CNⁱBu₂)₃phen (**8**). All of the three compounds are isostructural with their europium analogues.^{15,16,19} The central Ln(III) ion is octa-coordinated, and they all have a highly distorted dodecahedron geometry, with the dithiocarbamates behaving as bidentate ligands. For compound **2** (Figure 1), the average Sm–S and Sm–N bond distances are 2.87(6) and 2.56(1) Å, respectively. These are very close to the observed average values of Sm–S 2.87(7) and

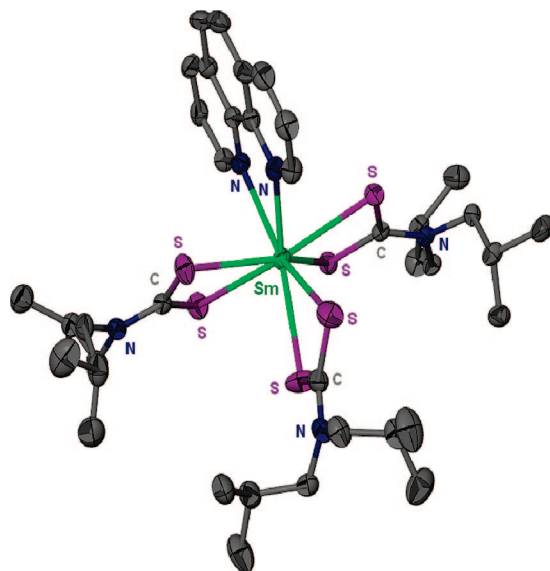


Figure 1. Molecular structure of [Sm(S₂CNⁱBu₂)₃phen], **2**. Hydrogen atoms and occluded solvent (acetonitrile) are omitted for clarity.

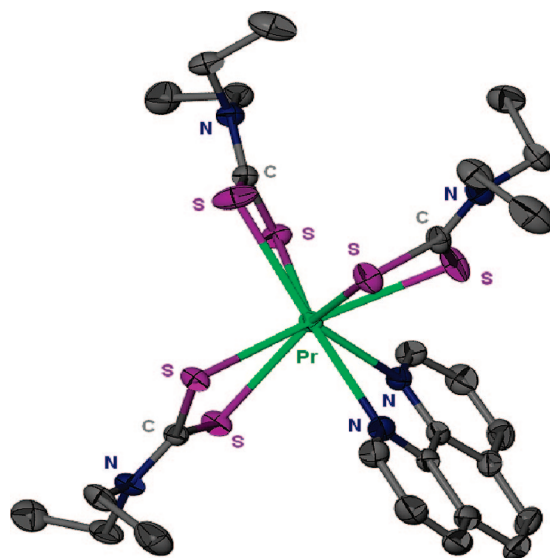


Figure 2. Molecular structure of [Pr(S₂CNEt₂)₃phen], **7**. Hydrogen atoms are omitted for clarity.

Sm–N 2.59(1) Å, which are previously reported for Sm(S₂CNEt₂)₃phen.¹⁵ The average S–Sm–S bite angle, which is 61.7(4)°, is also similar to that found in the latter (62.0(6)°). Compound **7** (Figure 2), on the other hand, has average Pr–S and Pr–N bond distances of 2.91(7) and 2.64(1) Å, respectively, which are comparable with the observed average values of Pr–S 2.90(5) and Pr–N 2.65(9) Å for the isostructural Pr(S₂CNEt₂)₃bipy.³¹ The average S–Pr–S bite angle of compound **7** and that of Pr(S₂CNEt₂)₃bipy are also closely similar, having values of 61.2(6)° and 61.39(2)°, respectively. Changing the alkyl group of the dithiocarbamate ligand from ethyl to isobutyl shows no significant effect on the Pr–S and Pr–N bond lengths and the S–Pr–S bite angle. For compound **8**, the average Pr–S and Pr–N bond distances are 2.91(4) and 2.65(1) Å, respectively, and the average S–Pr–S bite angle is 61.2(11)°. These values are very close to those observed for compound **7**. Changing the central lanthanide,

(31) Bower, J. F.; Cotton, S. A.; Fawcett, J.; Hughes, R. S.; Russell, D. R. *Polyhedron* **2003**, *22*, 347–354.

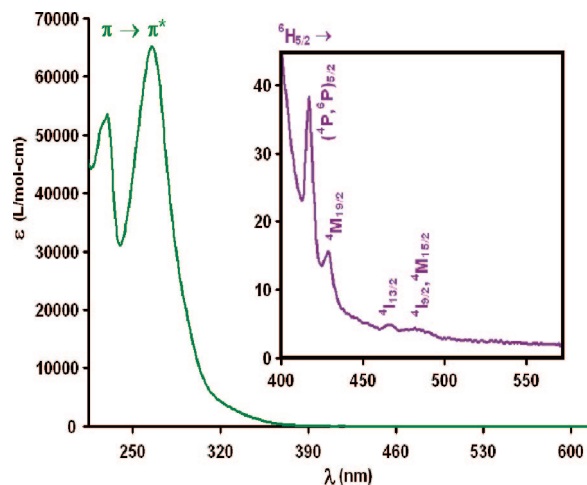


Figure 3. Electronic absorption spectrum of $[\text{Sm}(\text{S}_2\text{CNET}_2)_3\text{phen}]$ (**1**) in CH_3CN . The weak peaks corresponding to the $f-f$ transitions of Sm^{3+} are shown in the inset.

on the other hand, has significant effect on the Ln–S and Ln–N bond distances. Comparison of the average Ln–S bond distances of compounds **2** and **8**, both having the general formula $\text{Ln}(\text{S}_2\text{CN}^i\text{Bu}_2)_3\text{phen}$, shows a decrease in bond length from Pr–S 2.91(4) to Sm–S 2.87(6) Å. A similar decrease is observed for Ln–N bond distances (Pr–N 2.65(1) > Sm–N 2.56(1) Å). These observations are consistent with the fact that Sm^{3+} has a smaller ionic radius than Pr^{3+} due to the lanthanide contraction.

The crystal structures of several anionic lanthanide dithiocarbamate complexes, $[\text{Ln}(\text{S}_2\text{CNR}_2)_4]^-$, have been previously published. For R = Et, the structure for the salts of Na^+ and NH_2Et_2^+ with Ln = La have been reported. Both possess monoclinic symmetry and have the LnS_8 core, with a distorted dodecahedral configuration around the lanthanide.^{13,32} The tetrakis series with the cation NEt_4^+ for $[\text{Ln}(\text{S}_2\text{CNET}_2)_4]^-$, Ln = La–Lu (except Pm), have been found to be isostructural ($P2_1/c$) based on X-ray powder diffraction analysis, which suggests that the size of the metal does not alter the coordination environment.¹⁰ On the basis of the similarities of these structures and the consistency we have found for the $\text{Ln}(\text{S}_2\text{CNET}_2)_3\text{phen}$ compounds (Ln = Pr, Nd, Sm, Eu, Gd, Ho, Er),¹⁵ we anticipate that the NH_2Et_2^+ salt of $[\text{Ln}(\text{S}_2\text{CNET}_2)_4]^-$ for Ln = Pr and Sm share the same structure type as those previously described, although we are currently working to obtain the crystal structure of these compounds. In addition, the ^1H NMR, vibrational, and electronic spectra are consistent with the structures previously described.

Electronic Absorption Spectra. Figures 3 and 4 show the absorption spectra of compounds **1** and **7**, respectively. The spectra shown are representative of those of the other Sm^{3+} and Pr^{3+} dithiocarbamate complexes that were synthesized, having slight variations in the peaks observed in the UV region. For the mixed-ligand complexes, $\text{Ln}(\text{S}_2\text{CNR}_2)_3\text{L}$, the strong absorption bands situated in the UV region are centered at 229 ± 4 nm ($\epsilon \sim 5 \times 10^4$) and

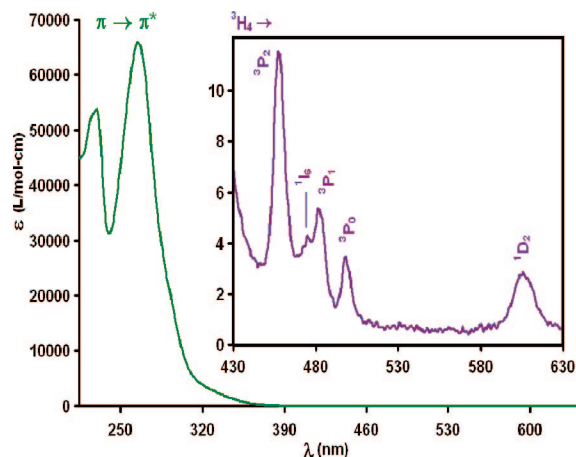


Figure 4. Electronic absorption spectrum of $[\text{Pr}(\text{S}_2\text{CNET}_2)_3\text{phen}]$ (**7**) in CH_3CN . The weak peaks corresponding to the $f-f$ transitions of Pr^{3+} are shown in the inset.

266 ± 3 nm ($\epsilon \sim 6.5 \times 10^4$) for the complexes where L = phen, 244 ± 1 nm ($\epsilon \sim 3 \times 10^4$) and 265 ± 2 nm ($\epsilon \sim 5 \times 10^4$) for L = bipy, and 233 ± 1 nm ($\epsilon \sim 5 \times 10^4$) and 267 ± 1 nm ($\epsilon \sim 6.5 \times 10^4$) for L = cphen. The first band (shorter-wavelength band) in each of the spectra is attributed to the π to π^* transitions of the bidentate aromatic ligand, L. The very intense band at 265–267 nm is a result of the overlapping absorption peaks of the aromatic ligands and the NCS_2 chromophore of the dithiocarbamate ligand. The characteristic NCS_2 absorption band is present at around 260.5 nm ($\epsilon \sim 1.7 \times 10^4$) in the diethyldithiocarbamate complex of Zn^{2+} , $\text{Zn}(\text{S}_2\text{CNET}_2)_2$.³³ For $[\text{Ln}(\text{S}_2\text{CNET}_2)_4]^-$, this band is observed at 266 ± 2 nm ($\epsilon \sim 4 \times 10^4$).

In the visible region, a number of very weak and narrow peaks (characteristic of the Laporte-forbidden $f-f$ transitions of the Ln^{3+} ions) are observed. Peak assignments were made by comparison with the spectra of the Ln^{3+} ions in halide lattices (LaCl_3 and LaF_3) and with the spectra of the Ln^{3+} aquo ions in dilute acid solution.^{34,35} For the Sm^{3+} complexes, the observed $f-f$ transition bands correspond to transitions from the ground state $^6\text{H}_{5/2}$ to the excited states $^4\text{P}_{5/2} + ^6\text{P}_{5/2}$ (417 ± 2 nm), $^4\text{M}_{19/2}$ (429 ± 2 nm), $^4\text{I}_{13/2}$ (467 ± 1 nm), and $^4\text{I}_{9/2} + ^4\text{M}_{15/2}$ (482 ± 1 nm). On the other hand, the peaks observed for the Pr^{3+} complexes are attributed to transitions from the ground state $^3\text{H}_4$ to $^3\text{P}_2$ (458 ± 1 nm), $^1\text{I}_6$ (476 ± 3 nm), $^3\text{P}_1$ (483 ± 2 nm), $^3\text{P}_0$ (499 ± 1 nm), and $^1\text{D}_2$ (607 ± 1 nm) states. It is interesting to note that the small but evident peak that corresponds to the $^3\text{H}_4 \rightarrow ^1\text{I}_6$ transition found in the spectra of the Pr^{3+} complexes is hardly observable in the spectra of the Pr^{3+} aquo ion.¹¹ This particular transition is hypersensitive to the environment about the Pr^{3+} ion.

The spectra of the complexes show a general red shift of the $f-f$ spectral bands in comparison with those of their corresponding ions in crystals and of their corresponding aquo ions. These red shifts are due to the nephelauxetic effect

(33) Koch, H. P. *J. Chem. Soc.* **1949**, 401–408.

(34) Carnall, W. T.; Fields, P. R.; Rajnak, K. *J. Chem. Phys.* **1968**, *49*, 4424–4442.

(35) Dieke, G. H. *Spectra and Energy Levels of Rare Earth Ions in Crystals*; Interscience: New York, 1968.

(32) Tang, N.; Zhu, H.; Tan, M.; Gan, X.; Wang, X. *Acta Chim. Sin.* **1991**, *49*, 42–47.

and are regarded as a measure of covalency of bonding between the metal and the ligands. The spectroscopic covalent parameters of the Ln(III)-ligand bonds, such as the nephelauxetic ratio (β), Sinha's parameter (δ), and bonding parameter ($b^{1/2}$) were calculated for the complexes studied, and these are shown in Table 1. The nephelauxetic ratio is generally measured in terms of the interelectronic repulsion parameters (Slater–Condon and Racah parameters), but since the magnitude of the nephelauxetic effect is small in lanthanide complexes, β is frequently approximated as the ratio of the wavenumber of the f–f transitions in the spectra of the complex and the free ion.³⁶ As the energy levels in the lanthanide free ions are not known, the spectra of the lanthanide aquo ions are used as standards. The closer β is to 1, the more ionic the bonding, but the lower the value, the more electron density is delocalized which indicates increasing bond covalency. The terms δ and $b^{1/2}$ are a measure of the extent of 4f–ligand mixing and are directly related to the magnitude of the nephelauxetic effect ($1 - \beta$). A more positive value signifies a greater degree of covalency in the complex.^{37,38} We have observed lower β values (higher δ and $b^{1/2}$) for the Pr³⁺ dithiocarbamates as compared to those of their Sm³⁺ analogues, suggesting a decrease in covalent character of the Ln–ligand bond in the heavier lanthanide complexes. This is consistent with that observed by Su and co-workers for the complexes Pr(S₂CNEt₂)₃phen ($\beta = 0.9757$) and Sm(S₂CNEt₂)₃phen ($\beta = 0.9958$).¹⁶ For both the Pr³⁺ and Sm³⁺ dithiocarbamates, the tetrakis complex gave peaks that are 2–4 nm red-shifted from those of the mixed-ligand complexes indicating a greater covalency in its Ln–ligand bonds. This reflects the higher polarizability of the sulfur atoms in the dithiocarbamate ligand relative to the nitrogen atoms in the bidentate aromatic amine, L. Changing the alkyl group in the dithiocarbamate ligand and varying the bidentate aromatic amine have very little effect on the degree of covalency in the Ln–ligand bonds in these complexes.

Photoluminescence Spectra. Previous spectroscopic studies of trivalent lanthanide chelates have revealed that the general mechanism of the sensitization of lanthanide ion luminescence via the “antenna effect” involves the following steps: (1) UV absorption of the organic chromophore resulting in excitation to the first excited singlet state ($S_0 \rightarrow S_1$); (2) nonradiative intersystem crossing from the singlet to the triplet state ($S_1 \rightarrow T_1$); (3) intramolecular energy transfer from the ligand-centered triplet state to the excited 4f states of the lanthanide ion; and (4) radiative transition from the lanthanide ion emissive states to lower energy states resulting in characteristic lanthanide emission.^{4,39} This, however, is a simplified model as the energy transfer involves numerous rate constants associated with each step (S_0 to S_1 , S_1 to T_1 , S_1 to Ln(III), T_1 to Ln(III), Ln(III) to T_1 as well as nonradiative deactivation steps).²⁹ Intersystem crossing

becomes quite favorable due to spin–orbit coupling induced by the heavy lanthanide metal. We do not observe ligand fluorescence in our complexes, so we assume there is little direct energy transfer to the metal from the singlet state.

The efficiency of the third step is crucial for the sensitization of lanthanide luminescence since the lanthanide ion emissive states must be efficiently populated for emission to occur. It is therefore necessary that there exists a suitable energy gap between the ligand-centered triplet state and the lanthanide ion emissive states. As first reported by Sato and Wada, the luminescence yield for Eu³⁺ complexes shows a maximum for the proper energy difference between the ligand-localized triplet state and the lanthanide emissive state.^{8,40} The gap must not be too large, to ensure a good overlap between the donor and acceptor energy levels, but it should not be too small (to prevent nonradiative deactivation via a back-energy transfer process from competing with lanthanide emission). The efficiency of the energy transfer can be determined by the phosphorescence lifetime of the lanthanide complex, vide infra, and can be understood in terms of the relative energies of the triplet states of the ligands.

In order to determine the triplet energy levels of rare earth chelates, it is common practice to use analogous chelates of a nonemitting lanthanide ion (i.e., La³⁺, Gd³⁺, and Lu³⁺). The f⁰ and f¹⁴ electronic configurations of La³⁺ and Lu³⁺, respectively, result in no f–f transitions for these lanthanides. In the case of Gd³⁺, the emitting energy level of this ion ($\sim 32\,000\text{ cm}^{-1}$)³⁵ is so much higher than the triplet state of organic ligands that energy transfer is not possible. The organic triplet state will thus deactivate through radiative transition to the ground-state resulting in molecular phosphorescence. With the absence of the lanthanide characteristic f–f emission, the emission spectra of the complexes of these lanthanides exhibit only the phosphorescence bands corresponding to the ligand-centered triplet energy levels. Since the energy of the ligand-centered triplet state does not depend significantly on the metal, we can use the Ln(S₂CNR₂)₃L and Ln(S₂CNEt₂)₄[−] complexes of these nonemitting lanthanides to measure the 0–0 transition and obtain the lowest triplet state energy of analogous Ln³⁺ chelates. For this reason, we have synthesized the Gd³⁺ analogues of the complexes under study as well as the La³⁺ analogue of the tetrakis complex.

Ligand Triplet Energy States. The shortest-wavelength phosphorescence band in the phosphorescence spectra of the La³⁺ and Gd³⁺ analogues was assumed to be the 0–0 transition, from which the energy of the lowest triplet state, T₁, was determined (Table 2).⁴¹ The triplet state of the dithiocarbamate ligand was determined from the emission spectra of the tetrakis complexes, NH₂Et₂[Gd(S₂CNEt₂)₄] and NH₂Et₂[La(S₂CNEt₂)₄] (Figure S1 in Supporting Information). Both complexes gave an emission at 433 nm (23 095 cm^{−1}), and this was taken as the T₁ of the diethyldithiocar-

(36) Jorgensen, C. K. *Prog. Inorg. Chem.* **1962**, *4*, 73.

(37) Sinha, S. P. *Spectrochim. Acta* **1966**, *22*, 57.

(38) Henrie, D. E.; Choppin, G. R. *J. Chem. Phys.* **1968**, *49*, 477.

(39) Crosby, G. A.; Whan, R. E.; Alire, R. M. *J. Chem. Phys.* **1961**, *34*, 743–748.

(40) Yang, Y. S.; Gong, M. L.; Li, Y. Y.; Lei, H. Y.; Wu, S. L. *J. Alloys Comp.* **1994**, *207–208*, 112–114.

(41) Sager, W. F.; Filipescu, N.; Serafin, F. A. *J. Phys. Chem.* **1965**, *69*, 1092–1100.

Table 2. Lowest Triplet Energy Levels Determined from the Low Temperature Phosphorescence Spectra of the Gd(III) and La(III) Analogues

	$E(T_1)$, cm^{-1}
Gd(S ₂ CNEt ₂) ₃ phen	22222 ± 49
Gd(S ₂ CN ^t Bu ₂) ₃ phen	22026 ± 98
Gd(S ₂ CNBz ₂) ₃ phen	21882 ± 48
Gd(S ₂ CNEt ₂) ₃ bipy	22727 ± 52
Gd(S ₂ CNEt ₂) ₃ cphen	21142 ± 45
[Gd(S ₂ CNEt ₂) ₄] ⁻	23095 ± 53
[La(S ₂ CNEt ₂) ₄] ⁻	23095 ± 107

bamate ligand. In the case of the mixed-ligand complexes, Gd(S₂CNR₂)₃L, three well-defined phosphorescence bands are observed, and none of them reflects transitions from the dithiocarbamate ligand (Figure S2). However, comparison of the phosphorescence spectra of the Gd(S₂CNR₂)₃phen complexes with that of the compound Gd(phen)₂Cl₃·2H₂O,⁴² which exhibits the phosphorescence of phenanthroline, shows similarity in their phosphorescence bands. These observations suggest that the intramolecular energy transfer to the emissive states of the lanthanide for the Ln(S₂CNR₂)₃L complexes is predominantly from the triplet state of the bidentate aromatic amine, L. This is not surprising given that L dominates the absorption spectra of the Ln(S₂CNR₂)₃L complexes and should influence the luminescence intensity greatly.

It was also observed that the lowest triplet energy state of the dithiocarbamate is higher in energy than those of the bidentate aromatic ligand, L. This is consistent with the fact that Gd(S₂CNR₂)₃L exhibits the phosphorescence of the bidentate L, rather than the higher energy dithiocarbamate. This also suggests that there may be intramolecular energy migration from the dithiocarbamate to the bidentate aromatic ligand.⁴² However, luminescence in the tetrakis compounds **6** and **12**, which do not have the bidentate aromatic amine, indicates that the dithiocarbamate ligand is also capable of sensitizing the lanthanide.

Lanthanide Substitutions. We have synthesized the Ln(S₂CNEt₂)₃phen complexes of Pr³⁺ and Sm³⁺ and compared their room temperature emission spectra (with identical concentrations) with those of the known, bright lanthanide emitters, Eu³⁺, Tb³⁺, and Dy³⁺ (Figure 5). The most intense emission was observed from the Sm³⁺ complex, which glows bright orange upon UV irradiation. The Pr³⁺ complex exhibits a weak red luminescence, but what is interesting is that it has a relatively brighter luminescence than the Eu³⁺, Tb³⁺, and Dy³⁺ analogues, which exhibit weak luminescence. This is unusual for Pr³⁺, which normally has internal quenching due to its many closely spaced excited states.⁴

The room temperature excitation (blue) and emission (red) spectra of the samarium complex **1** are shown in Figure 6. The excitation spectrum was obtained by monitoring the 646 nm line of the ⁴G_{5/2} → ⁶H_{9/2} emission. It contains a very intense broadband that corresponds to the excitation of the organic chromophore (S₀ → S₁) and several weak peaks corresponding to intraconfigurational f–f transitions from the ground-state of Sm³⁺. The ligand-localized transition

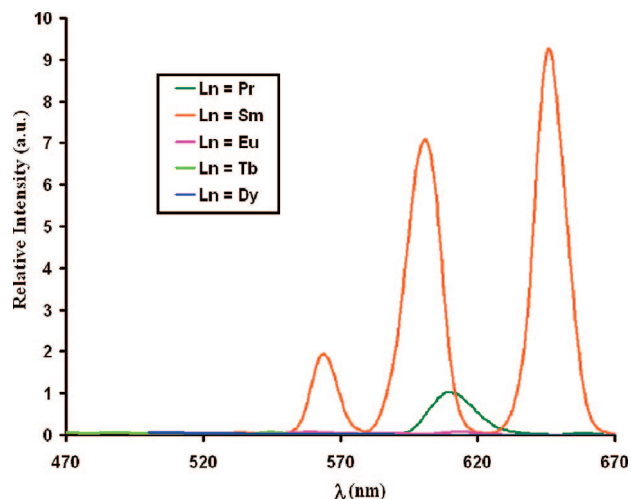


Figure 5. Emission spectra of [Ln(S₂CNEt₂)₃L] in CH₃CN at room temperature. Enhanced view of the emission spectra for Ln = Eu, Tb, and Dy are included in the Supporting Information. The wavelength corresponding to the S₀ → S₁ excitation band was used as the exciting wavelength (Sm 356 nm; Pr 362 nm; Eu 396 nm; Tb 337 nm; Dy 356 nm).

observed in the excitation spectrum was then used to obtain the emission spectrum, which shows four characteristic Sm³⁺ emission peaks. Three of these peaks originate from the Sm³⁺ lowest emitting state ⁴G_{5/2} and correspond to transitions to ⁶H_{9/2} (646 nm), ⁶H_{7/2} (601 nm), and ⁶H_{5/2} (564 nm) levels. The fourth peak, which is the least intense peak, corresponds to transition from a higher emissive state ⁴F_{3/2} to the ground state ⁶H_{5/2} (534 nm). The bright luminescence observed for the Sm(III) complex is reflective of a good match between the ligand-centered triplet state and the Sm³⁺ emissive states. As determined from the phosphorescence spectrum of Gd(S₂CNEt₂)₃phen, the lowest triplet state energy is 22 222 cm⁻¹. There are three Sm³⁺ excited states that can efficiently receive energy from the lowest triplet state, and these are the ⁴G_{7/2} (~20 050 cm⁻¹), ⁴F_{3/2} (~18 700 cm⁻¹), and ⁴G_{5/2} (~17 700 cm⁻¹) levels. Intense emission, however, is only observed from the ⁴G_{5/2} level. The reason for this is the close proximity of these three excited states to each other, which causes electrons from the higher states to rapidly relax to the ⁴G_{5/2} level, from which radiative transitions occur.⁴³

The room temperature excitation and emission spectra of the praseodymium compound **7** are shown in Figure 7. The 610 nm emission line was monitored to obtain the excitation spectrum, which consists of an intense ligand-centered transition band and several weak peaks corresponding to f–f transitions of Pr³⁺. Three peaks are found in the emission spectrum, which was recorded using the S₀ → S₁ excitation. The intense peak centered at 610 nm is mainly from the ¹D₂ → ³H₄ transition, but it is also believed to be overlapping with a much weaker peak corresponding to the ³P₀ → ³H₆ transition. The very weak emission peaks at 543 and 659 nm correspond to transitions from the ³P₀ emissive state to the ³H₅ and ³F₂ levels, respectively. Four excited states of Pr³⁺ lie close in energy to the phen-centered triplet state of the complex and these are the ¹I₆ (~21 000 cm⁻¹), ³P₁

(42) Yan, B.; Zhang, H. J.; Wang, S. B.; Ni, J. Z. *J. Photochem. Photobiol. A: Chem.* **1998**, *116*, 209–214.

(43) Zheng, Y.; Fu, L.; Zhou, Y.; Yu, J.; Yu, Y.; Wang, S.; Zhang, H. J. *Mater. Chem.* **2002**, *12*, 919–923.

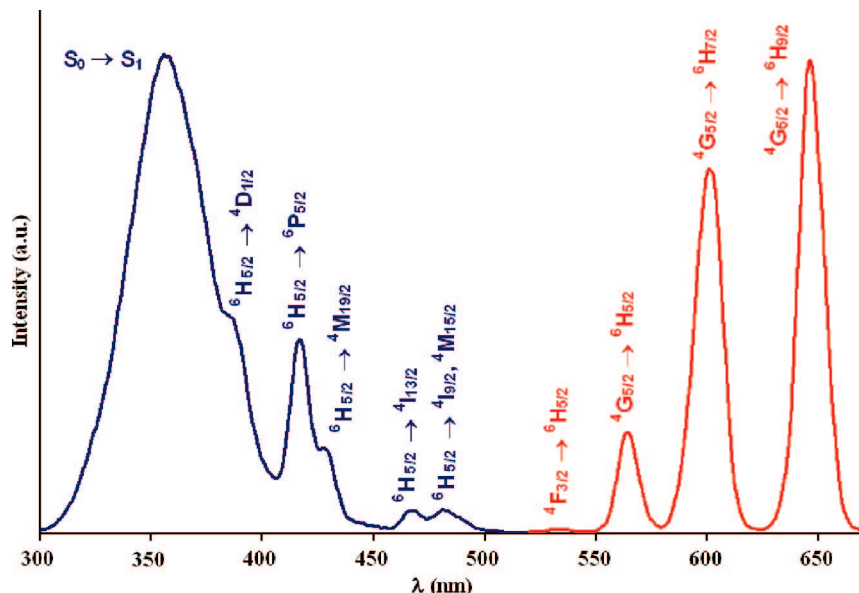


Figure 6. Excitation (blue) and emission (red) spectra of $\text{Sm}(\text{S}_2\text{CNEt}_2)_3\text{phen}$ (**1**) in CH_3CN at room temperature. The excitation spectrum was obtained by monitoring the 646 nm emission (${}^4\text{G}_{5/2} \rightarrow {}^6\text{H}_{9/2}$). The emission spectrum was recorded using the 356 nm excitation ($\text{S}_0 \rightarrow \text{S}_1$).

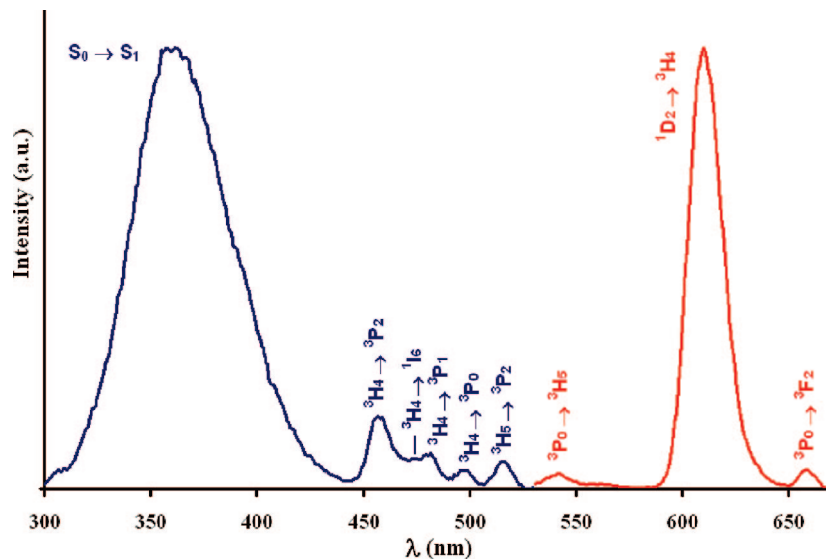


Figure 7. Excitation (blue) and emission (red) spectra of $\text{Pr}(\text{S}_2\text{CNEt}_2)_3\text{phen}$ (**7**) in CH_3CN at room temperature. The excitation spectrum was obtained by monitoring the 610 nm emission (${}^1\text{D}_2 \rightarrow {}^3\text{H}_4$). The emission spectrum was recorded using the 362 nm excitation ($\text{S}_0 \rightarrow \text{S}_1$).

($\sim 20\,800\text{ cm}^{-1}$), ${}^3\text{P}_0$ ($\sim 20\,050\text{ cm}^{-1}$), and ${}^1\text{D}_2$ ($\sim 16\,500\text{ cm}^{-1}$) states. A lower emissive state, ${}^1\text{G}_4$, exists at $\sim 10\,000\text{ cm}^{-1}$, but energy transfer to this state is not efficient since it is located far below the phen-localized triplet state of the complex. In most cases, emission originates mainly from the ${}^3\text{P}_0$ and ${}^1\text{D}_2$ levels as nonradiative relaxations from the ${}^1\text{I}_6$ and ${}^3\text{P}_1$ states to these lower energy levels occur. In a study by Voloshin et al., they have concluded that the emission properties of organic chelates of Pr(III) can be controlled depending on the position of the T_1 relative to the ${}^3\text{P}_0$ and ${}^1\text{D}_2$ emitting levels.⁴⁴ For complex **7**, where the T_1 is too close to ${}^3\text{P}_0$ but is in good match with ${}^1\text{D}_2$, the most intense emission comes from the ${}^1\text{D}_2$ level with very weak emission originating from the ${}^3\text{P}_0$ state.

In the room temperature excitation spectrum of the Eu^{3+} analogue (blue curve in Figure S3), it can be seen that the ligand-localized ($\text{S}_0 \rightarrow \text{S}_1$) excitation band is less intense than the ${}^7\text{F}_0 \rightarrow {}^5\text{D}_1$ excitation band. This indicates that the Eu^{3+} luminescence is not efficiently sensitized by the ligands. It has been previously reported that the maximum quantum yield for Eu^{3+} can be achieved when the triplet state of the ligand is in between the ${}^5\text{D}_2$ and ${}^5\text{D}_1$ levels of Eu^{3+} (in the range of $21\,500\text{--}22\,500\text{ cm}^{-1}$).⁴⁵ This explains why phenanthroline ($E(\text{T}_1) \sim 21\,500\text{ cm}^{-1}$)⁴⁶ is known to be a strong sensitizer to Eu^{3+} . But for the complex $\text{Eu}(\text{S}_2\text{CNEt}_2)_3\text{phen}$, the observed room temperature luminescence is not as intense

(44) Voloshin, A. I.; Shavaleev, N. M.; Kazakov, V. P. *J. Lumin.* **2001**, *93*, 199–204.

(45) Latva, M.; Takalo, H.; Mukkala, V.; Matachescu, C.; Rodriguez-Ubis, J. C.; Kankare, J. *J. Lumin.* **1997**, *75*, 149–169.

(46) Klink, S. I.; Hebbink, G. A.; Grave, L.; Oude Alink, P. G. B.; van Veggel, F. C. J. M.; Werts, M. H. V. *J. Phys. Chem. A* **2002**, *106*, 3681–3689.

Table 3. Luminescence Lifetime of Representative Sm(III) and Pr(III) Complexes ($\lambda_{\text{excitation}} = 337 \text{ nm}$)

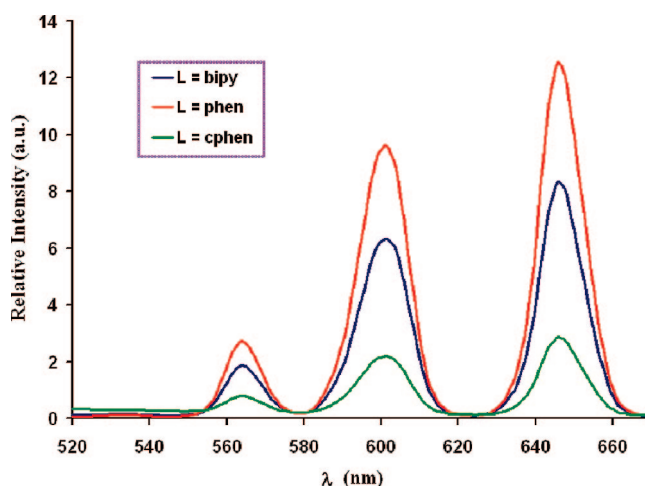
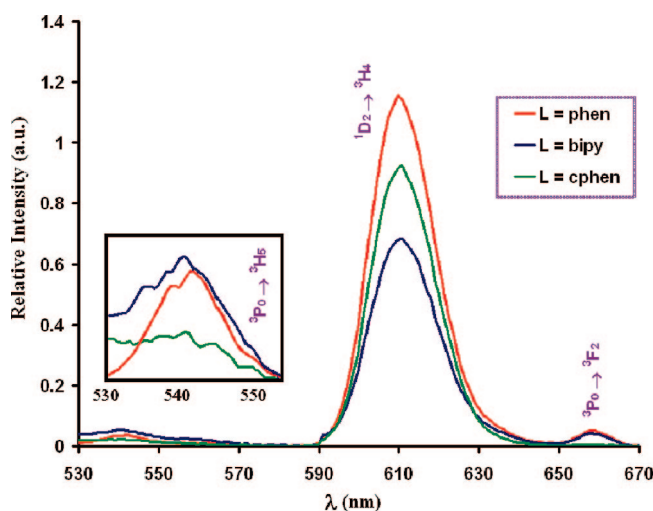
	$\lambda_{\text{emission}} \text{ (nm)}$	$\tau \text{ (}\mu\text{s)}$
Sm(S ₂ CNEt ₂) ₃ phen	646	20.0 ± 0.1
Pr(S ₂ CNEt ₂) ₃ phen	610	0.221 ± 0.002

as those of the other Eu(III)–phen systems. Although phenanthroline is a common antenna for the transfer of energy to Eu³⁺, a second ligand can significantly modify the luminescence properties.⁴² It has been recognized that the diminished luminescence is due to a ligand-to-metal charge transfer (LMCT) state that efficiently depopulates the Eu³⁺ emissive states.²⁸ The strong electron donating ability of the dithiocarbamate ligand and the strong tendency of Eu³⁺ to be reduced to Eu²⁺ are responsible for the efficient LMCT process in dithiocarbamate complexes of Eu³⁺.

The excitation spectra of the Tb³⁺ and Dy³⁺ analogues are shown in Figures S4 and S5, respectively, and their emission spectra are shown in Figure S6. For both complexes, the S₀ → S₁ excitation band is very weak (much weaker than direct f–f excitation), which clearly indicates that the ligands do not efficiently sensitize the luminescence of Tb³⁺ and Dy³⁺ in these complexes. As a result, their emission peaks are far less intense relative to those of their Sm³⁺ and Pr³⁺ counterparts. The lack of bright emission observed for these compounds can be explained by the poor match between the lowest ligand-centered triplet state and the Tb³⁺ and Dy³⁺ main emissive states. For the Tb³⁺ complex, the ⁵D₄ resonance level (~20 500 cm⁻¹) lies lower in energy than the lowest triplet energy level, but the energy gap ($\Delta E \sim 1722 \text{ cm}^{-1}$) is too small that quenching by thermally activated Ln–ligand back-energy transfer becomes a major competing process. It was previously reported that a high luminescence quantum yield is unlikely to be observed when the energy difference between the T₁ of the ligand and the ⁵D₄ level of Tb³⁺ is less than about 1850 cm⁻¹.⁴⁵ The very small energy gap ($\Delta E \sim 1222 \text{ cm}^{-1}$) between the T₁ and the ⁴F_{9/2} emissive state (~21 000 cm⁻¹) of Dy³⁺ also explains the lack of bright emission for the Dy³⁺ complex.

Ligand Substitutions. In the excitation spectrum of each of the samarium and praseodymium complexes studied, the most intense band corresponds to the ligand-centered electronic transition, indicating that the ligands are efficient sensitizers of lanthanide luminescence in all of these complexes. Interestingly, direct metal excitation is also evident, though less intense.

As discussed earlier, the triplet state of the complexes Ln(S₂CNEt₂)₃L, where we vary the bidentate aromatic ligand L, is localized on the aromatic amine. It is therefore expected that varying L would alter the energy of the T₁, and depending on the location of the T₁ with respect to the lanthanide emissive states, the luminescence intensity may either be enhanced or quenched. In Table 2, we see that the energy of the lowest triplet state increases in the following order: T_{cphen} < T_{phen} < T_{bipy}. For the samarium complexes, the luminescence intensity increases as follows: cphen < bipy < phen (Figure 8). In the case of the praseodymium chelates, the peaks in their emission spectra do not follow the same

**Figure 8.** Emission spectra of compounds **1** (red), **4** (blue), and **5** (green) having the general formula [Sm(S₂CNEt₂)₃L] in CH₃CN at room temperature.**Figure 9.** Emission spectra of compounds **7** (red), **10** (blue), and **11** (green) having the general formula [Pr(S₂CNEt₂)₃L] in CH₃CN at room temperature. The inset shows an enhanced view of the weak ³P₀ → ³H₅ emission peaks subjected to baseline correction.

trend (Figure 9). This is because they originate from different Pr³⁺ emissive states. For the 610 nm peak, which mainly originates from the ¹D₂ level, the intensity increases in the following order: bipy < cphen < phen. The weak peaks originating from the ³P₀ level, on the other hand, follow this order: cphen < bipy ~ phen.

The energy difference between the T₁ of the chelates and the relevant excited states of Sm³⁺ and Pr³⁺ are depicted in the energy level diagram shown in Figure 10. It can be seen that both the phen- and the bipy-localized T₁ (b and c in Figure 10) match well with the Pr³⁺ and Sm³⁺ excited states, and this is reflected on the ligand-sensitized luminescence observed for the complexes where L is phen or bipy. The emission, however, is generally more intense for the phen complexes as observed in the case of Sm³⁺ and the ¹D₂ emission peak of Pr³⁺. This agrees with the study by Yang et al. who reported that a higher luminescence yield is achieved in the presence of a more rigid planar structure, which decreases the probability of quenching by high-energy oscillators.⁴⁰ However, for the peaks originating from the

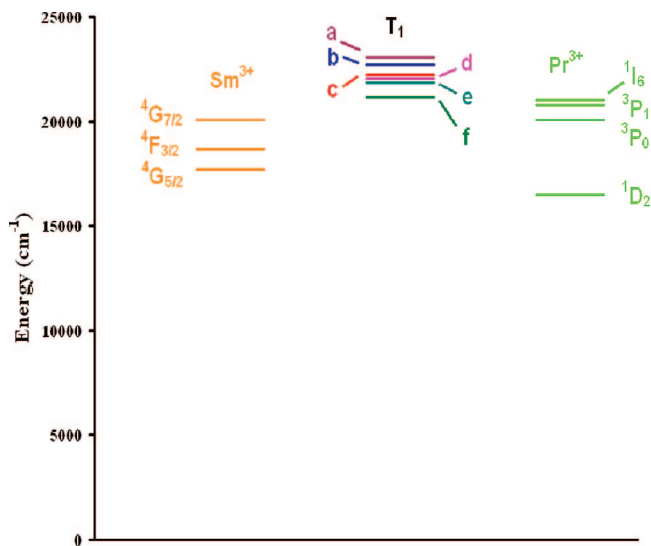


Figure 10. Energy level diagram featuring the lowest ligand-centered triplet state (T_1) of the chelates and the relevant Sm^{3+} and Pr^{3+} excited states. Chelates: (a) $[\text{Ln}(\text{S}_2\text{CNET}_2)_4]^-$; (b) $\text{Ln}(\text{S}_2\text{CNET}_2)_3\text{bipy}$; (c) $\text{Ln}(\text{S}_2\text{CNET}_2)_3\text{phen}$; (d) $\text{Ln}(\text{S}_2\text{CN}^i\text{Bu}_2)_3\text{phen}$; (e) $\text{Ln}(\text{S}_2\text{CNBz}_2)_3\text{phen}$; (f) $\text{Ln}(\text{S}_2\text{CNET}_2)_3\text{cphen}$.

$^3\text{P}_0$ level of Pr^{3+} , the intensity for the bipy complex is comparable to that of the phen analogue. This is because the higher T_{bipy} makes a better match with the energy of the $^3\text{P}_0$ excited state than the T_{phen} , which is too close to the $^3\text{P}_0$ level, and this offsets the decrease in intensity due to the less rigid bipy.

Chlorination of phenanthroline in the 5-position resulted in a decrease in the energy of the lowest triplet state by 1080 cm^{-1} . Although a suitable energy gap ($\Delta E \sim 3442\text{ cm}^{-1}$) exists between the cphen-localized T_1 (f in Figure 10) and the $^4\text{G}_{5/2}$ emitting state of Sm^{3+} , the very small gap ($\Delta E \sim 1092\text{ cm}^{-1}$) between the T_{cphen} and samarium's $^4\text{G}_{7/2}$ state promotes Ln–ligand back-energy transfer resulting in diminished luminescence for compound **5**. This is in agreement with the observations of Latva et al. in their study of the correlation between the T_1 of the ligand and Eu^{3+} quantum yield.⁴⁵ It was found that although the main emitting state of Eu^{3+} is the $^5\text{D}_0$ level, which is its lowest emissive state, the luminescence quantum yield is also affected by the proximity of the T_1 to higher excited states. A decrease in quantum yield was observed as the T_1 approaches either the $^5\text{D}_2$ or the $^5\text{D}_1$ level of Eu^{3+} . In the case of the Pr(III) complex **11**, it can be seen that chlorination of phenanthroline almost completely quenched the $^1\text{P}_0$ emission, and this is because of the very small gap between the T_{cphen} and the $^1\text{P}_0$ level. The $^1\text{D}_2$ emission, on the other hand, was not significantly affected, and this is due to the good match between the T_{cphen} and the $^1\text{D}_2$ level. These observations are consistent with what was reported by Voloshin et al. for Pr^{3+} chelates that conform to the energy term: $E(T_1) \approx E(^1\text{P}_0)$.⁴⁴

Varying the alkyl group of the dithiocarbamate ligand has no significant effect on the energy of the lowest triplet state (c, d, and e in Figure 10) owing to the fact that the T_1 is primarily localized on the bidentate aromatic ligand, L. In effect, the energy difference between the T_1 and the emissive states of the lanthanides are essentially the same for the

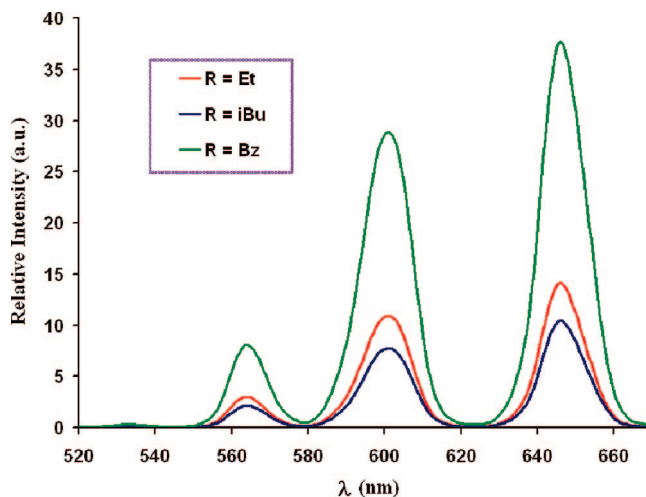


Figure 11. Emission spectra of compounds **1** (red), **2** (blue), and **3** (green) having the general formula $[\text{Sm}(\text{S}_2\text{CNR}_2)_3\text{phen}]$ in CH_3CN at room temperature.

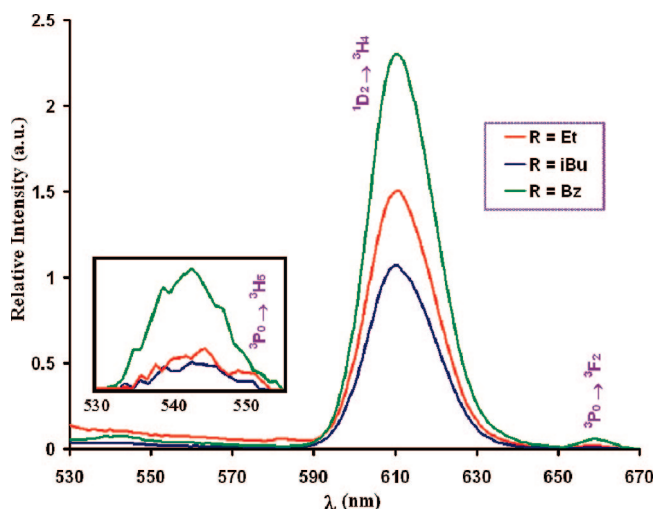


Figure 12. Emission spectra of compounds **7** (red), **8** (blue), and **9** (green) having the general formula $[\text{Pr}(\text{S}_2\text{CNR}_2)_3\text{phen}]$ in CHCl_3 at room temperature. The inset shows an enhanced view of the weak $^3\text{P}_0 \rightarrow ^3\text{H}_5$ emission peaks subjected to baseline correction.

complexes $\text{Ln}(\text{S}_2\text{CNR}_2)_3\text{phen}$ where R is ethyl, isobutyl, and benzyl. The luminescence intensity, however, changes dramatically particularly in the case of benzyl substitution, where the intensity is greatly enhanced (see Figures 11 and 12). In this case, the structure of the dithiocarbamate ligand plays a big role on the observed emission intensity. In going from ethyl to isobutyl, the number of high-energy C–H oscillators increases, and this leads to increased quenching of the lanthanide luminescence through coupling with C–H vibrations. The bulky benzyl substituent, on the other hand, not only has less deactivating vibrations but also protects the Ln^{3+} from solvent interaction, leading to an extremely enhanced luminescence. A number of studies have focused on designing ligands that are free of high-energy vibrations (by deuteration and halogenation)⁴⁷ and are capable of

(47) Hasegawa, Y.; Murakoshi, K.; Wada, Y.; Yanagida, S.; Kim, J.-H.; Nakashima, N.; Yamanaka, T. *Chem. Phys. Lett.* **1996**, *248*, 8–12.

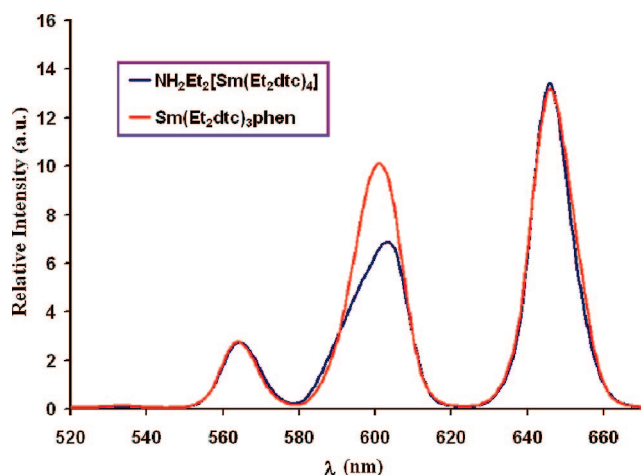


Figure 13. Emission spectra of compounds **1** (red) and **6** (blue) in CH_3CN at room temperature.

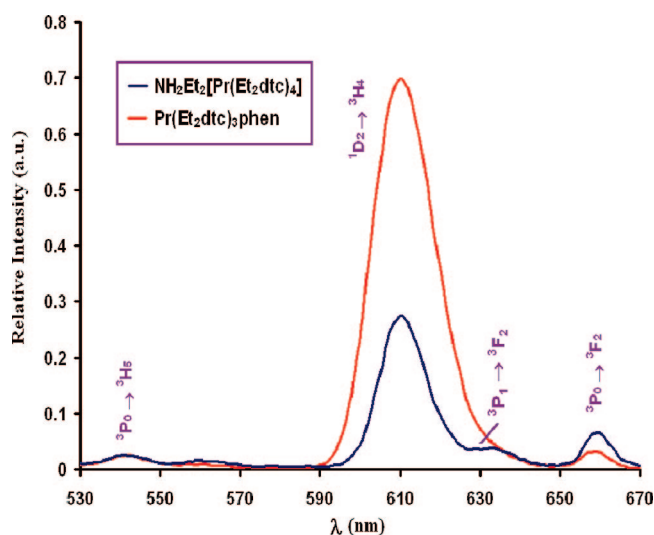


Figure 14. Emission spectra of compounds **7** (red) and **12** (blue) in CH_3CN at room temperature.

encapsulating the lanthanide ion (macrocyclic ligands)⁴⁸ to minimize vibration-induced nonradiative relaxations of the lanthanide.

For the homoleptic complexes, $[\text{Ln}(\text{S}_2\text{CNET}_2)_4]^-$, the T_1 is centered on the dithiocarbamate ligand and lies above the T_1 of the mixed-ligand complexes, which are primarily localized on the aromatic amine. Comparison of the luminescence intensity of $[\text{Ln}(\text{S}_2\text{CNET}_2)_4]^-$ and $\text{Ln}(\text{S}_2\text{CNET}_2)_3\text{phen}$ for $\text{Ln} = \text{Sm}$ and Pr are shown in Figures 13 and 14, respectively. For the $\text{Sm}(\text{III})$ complexes **1** and **6**, it can be seen that the intensity of the emission peaks are almost the same except for the ${}^4\text{G}_{5/2} \rightarrow {}^6\text{H}_{7/2}$ emission peak where a slightly reduced intensity is observed for the tetrakis complex **6**. It can also be seen that the band shape of this particular peak is distorted. Deconvolution of this peak revealed two maxima, one at 597 nm and the other at 605 nm, denoting that the ${}^6\text{H}_{7/2}$ level is split. Splitting is often indicative of reduced symmetry; however, the ligands appear to be equivalent based on the solution proton NMR. For the $\text{Pr}(\text{III})$

chelates **7** and **12**, it is observed that the intensity of the ${}^1\text{D}_2$ emission peak is reduced whereas the intensity of the ${}^3\text{P}_0$ emission peaks are enhanced for the tetrakis complex **12** relative to the mixed-ligand complex **7**. This is because the ${}^1\text{D}_2$ emissive state makes a better match with the T_1 of **7** ($\Delta E \sim 5722 \text{ cm}^{-1}$) than with the higher energy T_1 of **12** ($\Delta E \sim 6595 \text{ cm}^{-1}$). The ${}^3\text{P}_0$ emissive state, on the other hand, is too close to the T_1 of **7** ($\Delta E \sim 2172 \text{ cm}^{-1}$) but makes a good match with the T_1 of **12** ($\Delta E \sim 3045 \text{ cm}^{-1}$). Moreover, in the spectrum of **12**, a weak peak at around 429 nm, which corresponds to emission from the higher ${}^3\text{P}_1$ emissive state of Pr^{3+} , is evident and is a consequence of the higher T_1 of **12**.

Qualitatively, the luminescence intensities for the samarium and praseodymium complexes are clearly significantly higher than any of the other lanthanides studied. The luminescence quantum yield of the samarium compound **1** and the praseodymium compound **7** in anhydrous acetonitrile were determined relative to quinine bisulfate in 1 N H_2SO_4 ($\Phi = 54.6\%$).⁴⁹ Relative quantum yields of $11 \pm 2\%$ and $0.9 \pm 0.5\%$ were calculated for **1** and **7**, respectively. For comparison, the intrinsic quantum yield (calculated by the ratio between the radiative decay rate and the total decay rate) of the Eu^{3+} analogue was previously reported to be 4.2% at 300 K.²⁸ Although quinine has many advantages as a standard (it is not oxygen quenched, has no overlap between emission and excitation, and exhibits little concentration quenching), the emission wavelength is much lower than our complexes. But as plotted in Figure 5, comparison between the room temperature emission spectra of the two complexes discussed here and those of their Eu^{3+} , Tb^{3+} , and Dy^{3+} analogues clearly shows that the Sm^{3+} complex has the brightest luminescence, followed by the Pr^{3+} , and the others are close to the background.

Lifetime Measurements. The luminescence decay of compounds **1** and **7** were measured at room temperature in CH_3CN and these are shown in Figures S7 and S8, respectively. The luminescence lifetimes, τ , calculated from the decay curves are reported in Table 3. For both compounds, the most intense emission peak was monitored and these are the 646 nm ($\text{Sm}^{3+} {}^4\text{G}_{5/2} \rightarrow {}^6\text{H}_{9/2}$) and 610 nm ($\text{Pr}^{3+} {}^1\text{D}_2 \rightarrow {}^3\text{H}_4$) emission lines for **1** and **7**, respectively. The ${}^4\text{G}_{5/2}$ emission lifetime of the Sm^{3+} compound **1** is shorter than those reported for most complexes of Sm^{3+} with β -diketonate ligands⁵⁰ but is comparable with those observed for complexes of Sm^{3+} with iminodiacetic acid.⁵¹ The ${}^1\text{D}_2$ emission lifetime of the Pr^{3+} compound **7**, which is 221 ns, is almost similar to that reported for the octakis complex of Pr^{3+} with 3,4-lutidine *N*-oxide, $[\text{Pr}(\text{C}_7\text{H}_9\text{NO})_8](\text{ClO}_4)_3$, which is 224 ns.⁵²

(49) Melhuish, W. H. *J. Phys. Chem.* **1961**, *65*, 229–235.

(50) Brito, H. F.; Malta, O. L.; Felinto, M. C. F. C.; Teotonio, E. E. S.; Menezes, J. F. S.; Silva, C. F. B.; Tomiyama, C. S.; Carvalho, C. A. A. *J. Alloys Comp.* **2002**, *344*, 293–297.

(51) Hakala, H.; Liitti, P.; Puukka, K.; Peuralahti, J.; Loman, K.; Karvinen, J.; Ollikka, P.; Ylikoski, A.; Mulkala, V.; Hovinen, J. *Inorg. Chem. Commun.* **2002**, *5*, 1059–1062.

(52) Macalik, L.; Hanuza, J.; Hermanowicz, K.; Oganowski, W.; Ban-Oganowska, H. *J. Alloys Comp.* **2000**, *300–301*, 377–382.

(48) Sabbatini, N.; Guardigli, M.; Manet, I.; Ungaro, R.; Casnati, A.; Ziesse, R.; Ulrich, G.; Asfari, Z.; Lehn, J.-M. *Pure Appl. Chem.* **1995**, *67*, 135–140.

Conclusions

Due to the inherently weak luminescence of lanthanides, sensitization of their luminescence by organic ligands has been widely investigated. In this paper, we report the room temperature photoluminescence of homoleptic Sm³⁺ and Pr³⁺ dithiocarbamates, as well as their mixed-ligand complexes with aromatic bidentate amines. The suitability of the energy gap between the lowest excited ligand-localized triplet state and the metal-centered emissive states is a critical factor for the sensitization of lanthanide luminescence. Moreover, the molecular structure of the ligand should also be considered in designing highly emissive lanthanide complexes. Extremely enhanced lanthanide luminescence is observed with

the use of ligands having rigid planar structure and less high-energy oscillators.

Acknowledgment. We thank the National Science Foundation for funding this work (NER 0304273, CAREER 0449829).

Supporting Information Available: Additional synthetic procedures, low temperature phosphorescence spectra for the La³⁺ and Gd³⁺ complexes, room temperature photoluminescence spectra for the Eu³⁺, Tb³⁺, and Dy³⁺ complexes, and emission decay curves for **1** and **7**. This material is available free of charge via the Internet at <http://pubs.acs.org>.

IC701974Q